

Myeloma Genome Project Panel is a Comprehensive Targeted Genomics Panel for Molecular Profiling of Patients with Multiple Myeloma



Parvathi Sudha¹, Aarif Ahsan², Cody Ashby³, Tasneem Kausar², Akhil Khera⁴, Mohammad H. Kazeroun⁵, Chih-Chao Hsu², Lin Wang⁶, Evelyn Fitzsimons⁷, Outi Salminen⁵, Patrick Blaney⁸, Magdalena Czader⁶, Jonathan Williams⁴, Mohammad I. Abu Zaid¹, Naser Ansari-Pour⁵, Kwee L. Yong⁷, Frits van Rhee⁹, William E. Pierceall², Gareth J. Morgan⁸, Erin Flynt², Sarah Gooding^{4,5,10}, Rafat Abonour¹, Karthik Ramasamy^{4,10,11}, Anjan Thakurta^{2,10,11}, and Brian A. Walker¹

ABSTRACT

Purpose: We designed a comprehensive multiple myeloma targeted sequencing panel to identify common genomic abnormalities in a single assay and validated it against known standards.

Experimental Design: The panel comprised 228 genes/exons for mutations, 6 regions for translocations, and 56 regions for copy number abnormalities (CNA). Toward panel validation, targeted sequencing was conducted on 233 patient samples and further validated using clinical FISH (translocations), multiplex ligation probe analysis (MLPA; CNAs), whole-genome sequencing (WGS; CNAs, mutations, translocations), or droplet digital PCR (ddPCR) of known standards (mutations).

Results: Canonical immunoglobulin heavy chain translocations were detected in 43.2% of patients by sequencing, and aligned with FISH except for 1 patient. CNAs determined by sequencing and MLPA for 22 regions were comparable in 103 samples and concordance between platforms was $R^2 = 0.969$. Variant allele frequency (VAF) for 74 mutations were compared between sequencing and ddPCR with concordance of $R^2 = 0.9849$.

Conclusions: In summary, we have developed a targeted sequencing panel that is as robust or superior to FISH and WGS. This molecular panel is cost-effective, comprehensive, clinically actionable, and can be routinely deployed to assist risk stratification at diagnosis or posttreatment to guide sequencing of therapies.

Introduction

While personalized medicine in multiple myeloma is still in its infancy (1–11), next-generation sequencing (NGS) technologies have proven useful in identifying mutations, gene expression differences, and other key genetic events in multiple myeloma [refs. 12, 17; such as translocations and copy number abnormalities (CNA)] but so far their clinical utility has been limited (18). Despite efforts to use genomics to improve identification of patients with high-risk multiple myeloma, the detection of key translocations and CNA by FISH remains the standard in the clinic. Although FISH is the most frequently used technique across clinical diagnostic laboratories, there is a vast difference in the methodologies used including whether or not CD138⁺ cell selection is performed, regions of the genome probed, and limited interrogation of immunoglobulin heavy chain (IgH) locus rearrangements (19).

Other technologies, such as copy number arrays (20), and multiplex ligation-dependent probe amplification (MLPA; ref. 21) have also been used diagnostically to detect CNAs such as del(*CDKN2C*) on 1p, del(*TP53*) on 17p, and gain/amplification of *CKS1B* on 1q, which are associated with poor outcome. Together, the high-risk IgH translocations and del(*TP53*) are used to stratify high-risk patients according to the revised-ISS (R-ISS) criteria (22, 23). The addition of 1q gain or amplification, and *TP53* mutation have also been used to further stratify patients as high risk (24, 25). *MYC* rearrangements are associated with poor outcome in multiple myeloma but the presence of the rearrangements is not easy to detect, due to the complexity of rearrangements and the high number of partner loci (26, 27). FISH can be used to detect the t(8;14) *IgH-MYC* rearrangement, but this only accounts for a minority of the cases (27, 28). A more unbiased methodology is required to detect all possible rearrangements.

Recently, additional high-risk markers have been reported, including biallelic alterations in *TP53* or *DIS3*, arising from deletion or

¹Melvin and Bren Simon Comprehensive Cancer Center, Division of Hematology Oncology, Indiana University School of Medicine, Indiana University, Indianapolis, Indiana. ²Translational Medicine, Bristol Myers Squibb, Summit, New Jersey. ³Department of Biomedical Informatics, College of Medicine, University of Arkansas for Medical Sciences, Little Rock, Arkansas. ⁴Oxford University Hospitals NHS Foundation Trust, Oxford, United Kingdom. ⁵MRC Molecular Haematology Unit, MRC Weatherall Institute of Molecular Medicine, University of Oxford, Oxford, United Kingdom. ⁶Department of Pathology and Laboratory Research, Indiana University School of Medicine, Indiana University, Indianapolis, Indiana. ⁷Cancer Institute, University College London, London, United Kingdom. ⁸Perlmutter Cancer Center, NYU Langone Medical Center, New York, New York. ⁹Myeloma Center, Winthrop P. Rockefeller Cancer Institute, University of Arkansas for Medical Sciences, Little Rock, Arkansas. ¹⁰Oxford Center for Translational Myeloma Research, University of Oxford, Oxford, United Kingdom. ¹¹Radcliffe Department of Medicine, Medical Sciences Division, University of Oxford, Oxford, United Kingdom.

Note: Supplementary data for this article are available at Clinical Cancer Research Online (<http://clincancerres.aacrjournals.org/>).

P. Sudha, A. Ahsan, K. Ramasamy, A. Thakurta, and B.A. Walker contributed equally to this article.

Corresponding Authors: Brian A. Walker, Melvin and Bren Simon Comprehensive Cancer Center, Division of Hematology Oncology, Indiana University School of Medicine, Indiana University, 980 W Walnut St, Indianapolis, IN 46202. Phone: 317-278-7733; E-mail: bw75@iu.edu; and Anjan Thakurta, Radcliffe Department of Medicine, Medical Sciences Division, University of Oxford, Level 6, West Wing, John Radcliffe Hospital, Headington, Oxford OX3 9DU, United Kingdom. Phone: 908-514-5813; E-mail: AThakurta@outlook.com

Clin Cancer Res 2022;28:2854–64

doi: 10.1158/1078-0432.CCR-21-3695

This open access article is distributed under the Creative Commons Attribution-NonCommercial-NoDerivatives 4.0 International (CC BY-NC-ND 4.0) license.

©2022 The Authors; Published by the American Association for Cancer Research

Translational Relevance

Here we provide a validated panel for targeted sequencing and analysis of myeloma and other plasma cell dyscrasias to identify the common genomic abnormalities that are diagnostic, prognostic, and clinically actionable. This panel can identify the common immunoglobulin translocations and copy number abnormalities currently detected by FISH, as well as less common translocations, *MYC* rearrangements, and mutations that are not currently tested for in a standard manner. We hope that adoption of a common sequencing panel will improve patient diagnostics and can be used to assist in risk stratification at diagnosis or posttreatment to guide therapeutic decision making.

mutation of the remaining allele (25, 29–32). Newer patient segments such as Myeloma Genome Project (MGP) Double-Hit and Mayo Clinic (Rochester, MN) double- or triple-hit multiple myeloma identify patients with significant adverse prognosis (21, 24, 25) but their assessment is not widespread due to lack of availability of diagnostic tests.

Genomic risk stratification may also be extended to asymptomatic disease states of monoclonal gammopathy of undetermined significance and smoldering multiple myeloma (SMM). We and others have shown that IgH translocations, mutations in *NRAS*, *KRAS*, and *FAM46C*, as well as *MYC* translocations or abnormalities at 8q24 can define a high-risk group of patients with SMM who are likely to progress to multiple myeloma quickly, independent of current International Myeloma Working Group (IMWG) risk factors (33–35).

Here, we describe a comprehensive, cost-effective, hybridization capture-based, NGS assay panel for targeted sequencing of recurrently mutated key genes in newly diagnosed and relapsed multiple myeloma, genomic regions of CNA, translocations involving immunoglobulin (Ig) heavy and light chain loci, and *MYC* translocations. Previous versions of this panel have been used extensively in the research setting (1, 26, 27, 29, 30, 33, 36–39). We evaluated the current expanded and updated panel on 233 patient samples and extensively validated results using multiple comparative assays. A complete guidance document from laboratory methodology, capture design, bioinformatic pipeline, and analysis visualization tool has been made publicly available for others to utilize. The assay technology was transferred to a clinical diagnostic laboratory and its performance was compared with existing clinical diagnostic data. This newly developed, highly validated assay and platform enables rapid and reliable detection of patients with high-risk or therapeutically-targetable biomarkers and has the potential to guide risk-adapted treatment selection and sequencing as a personalized medicine strategy. Finally, we propose an engagement with the multiple myeloma community to consider available molecular profiling approaches including this panel to adopt an actionable strategy for diagnosis and treatment of patients with multiple myeloma.

Materials and Methods

Patients and samples

Patient material was obtained after written informed consent in accordance with the U.S. Common Rule and were approved by the Institutional Review Board. CD138⁺ plasma cells were magnetically sorted from bone marrow aspirates using the AutoMACS Pro (Miltenyi Biotec GmbH) or RoboSep (STEMCELL Technologies). The

postselection plasma cell purity was determined by flow cytometry using anti-CD45-ECD (Beckman Coulter), anti-CD138 (Becton Dickinson), and only samples with more than 85% purity were used in this study. DNA was isolated from CD138⁺ plasma cells using the AllPrep DNA/RNA or Puregene kits (Qiagen). DNA from peripheral blood, saliva, or CD34⁺ stem cells was isolated and used as a matched nontumor control where available. For 39 samples, the CD138⁻ fraction was used as the control sample. All DNA were eluted in low EDTA buffer.

Panel design

Based on the findings of the MGP(1) and other multiple myeloma genome sequencing studies (2–4, 7, 8, 17, 40, 41), prognostically and biologically relevant genes and genomic regions were identified (Supplementary Fig. S1). By utilizing this information, two capture panels were designed: one for common multiple myeloma translocations, and another for mutation and CNA information (Supplementary Tables S1–S3). The mutation and CNA probe set covers approximately 1.19 Mb of the genome. Probes capture exonic regions (including flanking 10 bp) of 228 key multiple myeloma genes for mutation detection. An additional 471 SNPs were captured to aid in copy number variation detection either within or surrounding key genes or in other areas of the genome. For example, in addition to the 10 exons captured for *TP53*, an extra 40 SNPs around *TP53* were included in the design for increased sensitivity to detect loss of the region. These SNPs were chosen with a population minor allele frequency > 0.35, and the change in B allele frequency between control and tumor samples was used in combination with read depth ratio to infer both deletions and gains. To avoid hybridization artifacts and low depth problems, SNPs in guanine cytosine (GC)-rich regions were excluded. For the mutation panel, 4,785 total regions were captured.

The translocation panel covers about 4.32 Mb of the genome. Tiling capture probes were designed to cover the V, D, and J segments as well as the entire constant region to identify Ig translocations. To detect *MYC* translocations and rearrangements, tiling probes were designed upstream and downstream of *MYC* (from *NSMCE2* to *GSDMC*). Some sequences were omitted due to mappability problems in repetitive regions which prevent sequence-specific probe design, meaning that the capture regions are not contiguous. The specifics of the captured region can be found in the annotation files at <https://github.com/bwalker2/Targeted-Panel-Analysis>.

For both the mutation and translocation panels, the probes were empirically balanced by testing on a set of eight saliva DNA samples using the HyperCap (KAPA Biosystems) reagents. Any over- or undercapture of regions on the panels were balanced out by modifying the amounts of probes for each region until a roughly uniform coverage of the regions of interest was observed. The catalog numbers of the mutation and translocation panels (v2.1) are IRN 1000008523 and IRN 1000008533 (KAPA Biosystems), respectively. Future updates to panel designs will be documented at <https://github.com/bwalker2>.

Samples were processed using HyperCap reagents as described in Supplementary Methods and validated accordingly (Supplementary Figs. S2–S10). Libraries were sequenced using 75 bp paired end reads, to a mean total depth of 344× (mutation panel 867×, translocation panel 252×).

Targeted panel data analysis

For all samples the same informatics pipeline was used. *bcl2fastq* was used for demultiplexing and Burrows-Wheeler Aligner (BWA) mem (v. 0.7.12) for alignment to University of California Santa Cruz's (GRCh37/hg19) human reference genome. Strelka (v.2.9.2) was used

for variant calling and single-nucleotide variants (SNV) were filtered using *fpfilter* (<https://github.com/ckandoth/variant-filter>) with a 5% variant allele frequency (VAF) cut-off. Indels were filtered using a 10% VAF cut-off. Variants were annotated using Variant Effect Predictor (v.101). To determine copy number, a normalized depth comparison between tumor and control samples was used and segments of SNP variance were utilized to identify regions of chromosomal deletion and gain. A Python library and command-line software toolkit, CNVKit (v 0.9.7) was used for copy number calling pipeline. Quality control (QC) metrics were calculated using Picard's (v 2.10.0) "CollectHsMetrics" command. Intra- and interchromosomal rearrangements were called using Manta (v1.6.0) with default settings and the exome flag specified. An SQLite database was generated using somatic variants by Strelka2, structural variants by Manta, copy number depth metrics by CNVKit, and QC metrics by Picard. Data were visualized using a custom built "RShiny" application, TarPan (42) showing the mutations, translocations, copy number, QC metrics, and cross-sample contamination estimations. In TarPan, copy number can be manually normalized based on the ratio and SNP allele calls using the best fitting chromosomes with the least variance (usually chromosome 2 or 10). A full pipeline is available at <https://github.com/bwalker2/Targeted-Panel-Analysis>.

Orthogonal technologies for validation

Orthogonal technologies were used to validate the results of the panel, including FISH, MLPA, and whole-genome sequencing (WGS). Details are provided in Supplementary Methods.

Data availability

The analytical methods generated in this study are available at <https://github.com/bwalker2/Targeted-Panel-Analysis>. Data have been submitted to the European Genome-Phenome Archive under accession numbers EGAD00001008689 and EGAD00001008735.

Results

Detection of key prognostic markers and risk stratification of patients

The targeted capture panel was tested on 233 samples from 190 patients with SMM ($n = 9$), multiple myeloma [$n = 221$, of which 138 were newly diagnosed multiple myeloma (NDMM)], and plasma cell leukemia (PCL; $n = 3$). Mutations, translocations, and CNAs were determined using a standard computational pipeline. In agreement with previous studies, we identified key mutations including *KRAS* (25%), *NRAS* (15%), *DIS3* (12%), *FAM46C* (5%), *BRAF* (11%), and *TP53* (12%). The frequency of 63 previously identified driver genes from MGP(1) in our dataset are shown in Fig. 1, along with identified key cytogenetic groups and CNAs. Notably, with the exception of *SAMHD1*, all other driver gene mutations were detected. Thus, the current panel is able to detect most of the driver genes identified thus far in NDMM, including in six genes commonly mutated in relapse refractory multiple myeloma (N. Ansari-Pour; unpublished data).

Poor prognostic CNA markers in multiple myeloma include del1p (*CDKN2C*), gain/amp 1q (*CKS1B*), and del17p (*TP53*). In this dataset, deletion of *CDKN2C* was identified in 30 samples (12.8%) including homozygous deletion in 7 samples. Copy number-neutral LOH (CNN-LOH) was detected in an additional 5 samples. There was no significant difference in frequency of deletion of *CDKN2C* among the disease states. Gain (3 copies) or amplification (4+ copies) of 1q (*CKS1B*) was detected in 81 samples (34.8%), of which 11 were amplifications. Gain/amp 1q was detected in 62.5% SMM, 31.9%

NDMM, 33.7% previously treated multiple myeloma, and 66.6% PCL with no significant difference between groups. Deletion of *TP53* was detected in 36 samples (15.5%), including homozygous deletion in 6 samples. CNN-LOH was detected in an additional six samples. There was a significant increase in frequency of *TP53* deletion between NDMM and previously treated multiple myeloma ($P = 0.026$): 11.6% versus 22.9%.

We applied genomic risk stratification criteria to the samples, exploring MGP Double-Hit, biallelic *TP53*, and Mayo Clinic risk classification (Fig. 1), which requires *TP53* mutation status in addition to deletion (24, 25). MGP Double-Hit (biallelic *TP53* abnormalities or gain 1q with ISS III) was applied to NDMM samples and identified 10.9% (15/138) of patients. Biallelic *TP53* abnormalities were detected in 9.9% of samples; 9 of 138 (6.5%) were NDMM, 13 of 83 (15.7%) were previously treated, and 1 of 3 (33.3%) was PCL, and none in SMM. There was a significant increase in biallelic *TP53* events from diagnosis to those previously treated ($P = 0.015$).

The Mayo Clinic risk classification, where t(4;14), t(14;16), t(14;20), gain 1q, del(17p), or mutation of *TP53* are considered high-risk markers and are additive, was applied to all multiple myeloma samples identifying 90 of 221 standard risk, 72 of 221 high risk, 38 of 221 double hit, and 9 triple-hit multiple myeloma. Of these, the split between NDMM and previously treated multiple myeloma was 42.7% versus 37.3% standard, 34.8% versus 28.9% high, 15.2% versus 20.4% double, and 0.7% versus 9.6% triple hit. There was a significant increase in triple-hit multiple myeloma in previously treated patients ($P = 0.0011$) and all but one of the triple-hit patients had biallelic *TP53* abnormalities.

Mutation detection and validation

Of the 233 samples, WGS mutation data were available for 113. For this analysis, WGS data were considered only for regions captured by the mutation panel and further filtered for those with a protein coding effect. There were 379 variants detected that passed filtering by both sequencing methods. A comparison of VAFs between sequencing methods showed a correlation of $R^2 = 0.9006$ (Fig. 2A).

Mutation detection validation was performed using samples with known VAF for common mutations. Five DNA standards (Horizon Discovery; Supplementary Table S4) were used which had mutations at frequencies from 1.3% to 40% VAF engineered into them in key genes important in cancer. The VAF of the DNA standards is commercially determined by ddPCR and can be used to show that the mutations are detected at the correct frequency and that the bioinformatics pipeline is able to annotate them correctly. From these five standards, 74 mutations were assayed on the panel. The expected and observed VAF for each mutation were plotted giving a correlation coefficient of $R^2 = 0.9849$ (Fig. 2B), indicating high concordance of results.

CNA validation

CNA was determined by targeted sequencing and by MLPA for 22 regions that were directly comparable. Initial validation of MLPA and sequencing was performed in a panel of 13 multiple myeloma cell lines. For all the 22 regions combined, a concordance of 99.61% was observed between MLPA and sequencing in the 13 cell lines (Fig. 3A; Supplementary Table S5; Supplementary Fig. S4). In 101 patient samples the concordance between the technologies was $R^2 = 0.987$ (Fig. 3B). For the important prognostic regions, the concordance was $R^2 = 0.962$ (*CDKN2C*), $R^2 = 0.986$ (*CKS1B*), and $R^2 = 0.973$ (*TP53*; Fig. 3C-E).

We compared the copy number determination between WGS and panel sequencing methods for the common prognostic regions, *CDKN2C*, *CKS1B*, *TP53*, and *RB1* (Supplementary Tables S6-S10).

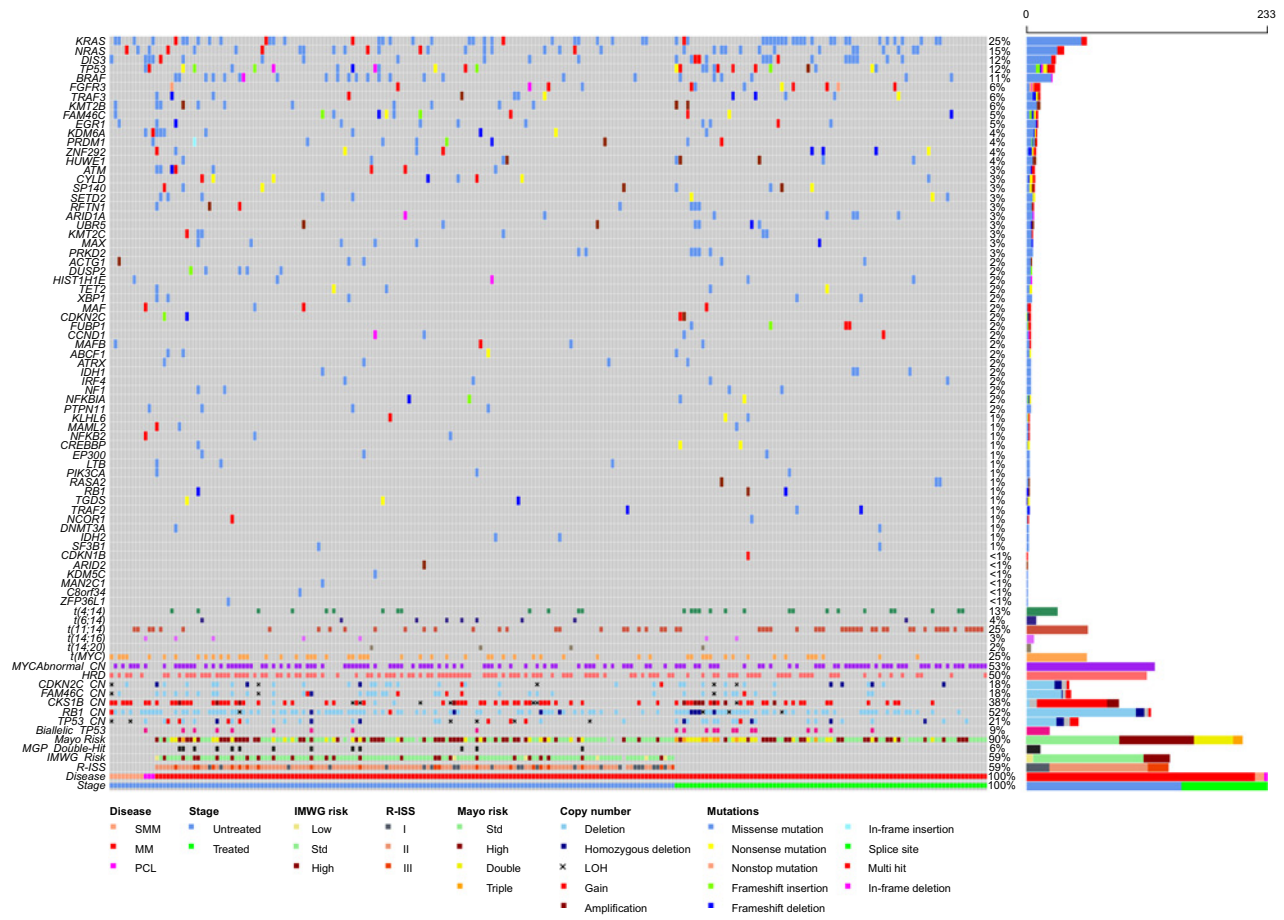


Figure 1. Frequency of mutations in 63 key driver genes, translocations, hyperdiploidy, and key CNAs detected by targeted sequencing. Risk stratification of patients was determined from genomic and biochemical markers. MM, multiple myeloma; Std, standard.

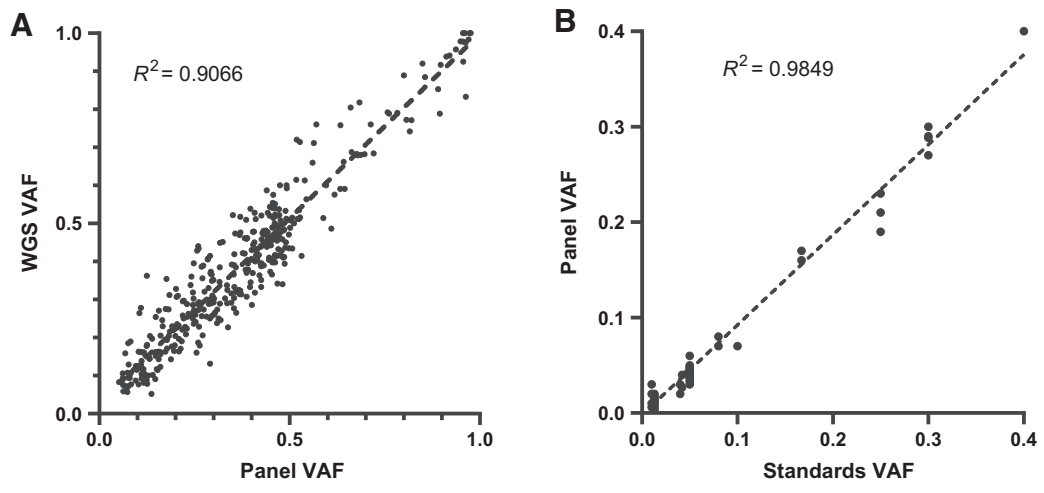
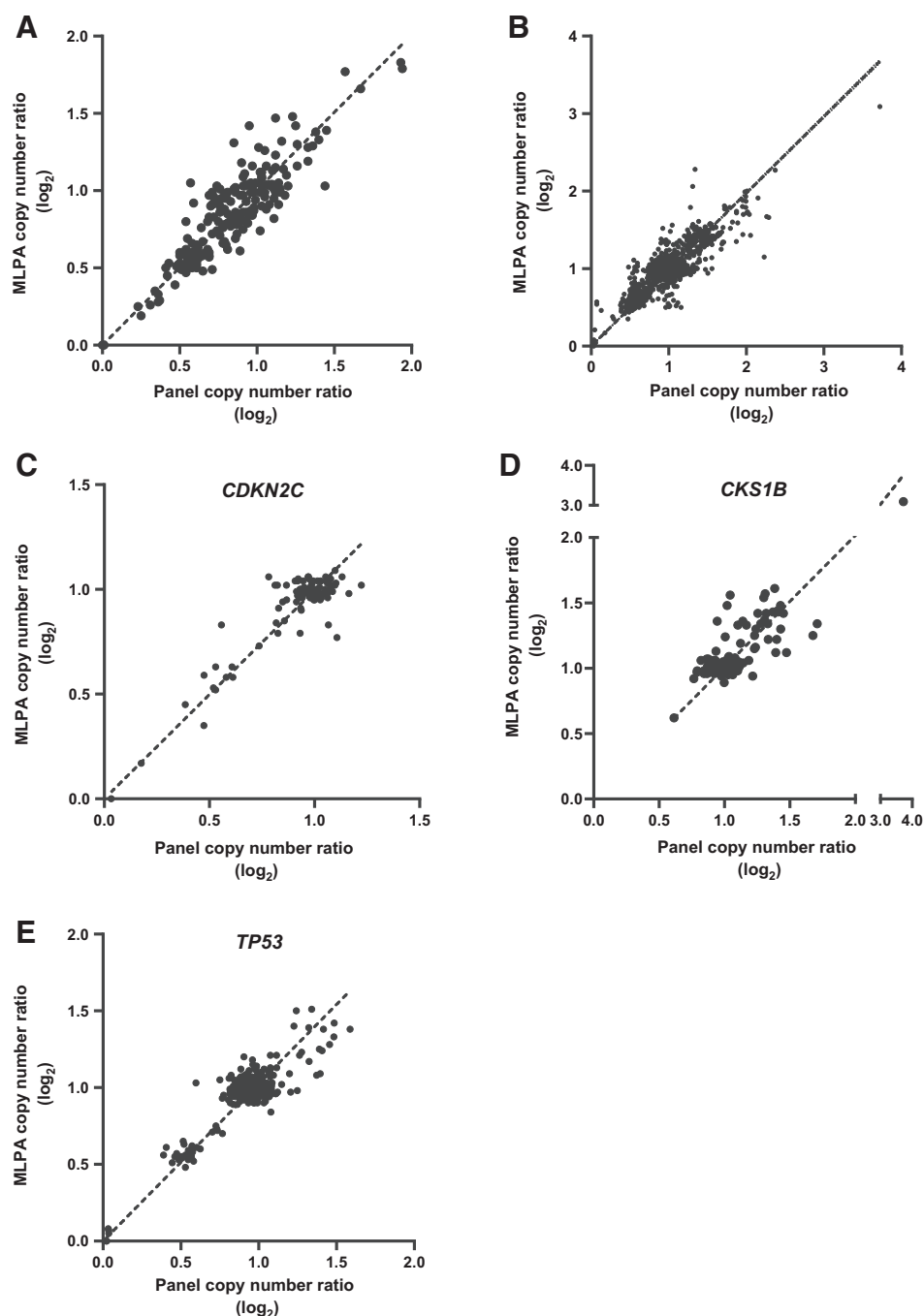


Figure 2. Validation of mutation VAF against matched WGS data (A) and DNA standards (B).

Downloaded from <http://aacrjournals.org/clinccancerres/article-pdf/28/13/2854/175669/2854.pdf> by guest on 04 August 2022

**Figure 3.**

Validation of copy number against MLPA. Copy number ratio (\log_2) was determined for 13 multiple myeloma cell lines by targeted panel sequencing and MLPA (A). Comparison of copy number ratio for multiple myeloma 101 patient samples for 22 common regions (B), with emphasis on regions associated with poor prognosis including *CDKN2C* (C), *CKS1B* (D), and *TP53* (E).

At *CDKN2C*, a deletion (0 or 1 copies) was detected in 11 of 113 samples on the panel and matched with WGS data. For *CKS1B*, gain/amplification (≥ 3 copies) was detected in 46 of 113 samples, of which one was not detected by WGS. WGS did detect gain of *CKS1B* in one sample that was not detected by the panel. For *RBI1*, deletion was detected in 55 of 113 samples by the panel and agreed with WGS data. For *TP53*, deletions were detected in 21 of 113 samples by both the panel and WGS. The sensitivity, specificity, positive predictive value (PPV), negative predictive value (NPV), and accuracy for each region are shown in **Table 1**. All PPVs and NPVs were above 95%.

By combining all the data from these four loci, the overall performance of the assay for CNA detection, compared with WGS, was calculated: sensitivity (99.25%), specificity (99.38%), PPV (98.52%), NPV (99.69%), and accuracy (99.34%).

Detection of small homozygous deletions in *CDKN2C*, *RBI1*, and *TP53*

To further explore the utility of the panel, we examined homozygous deletions of the key tumor suppressor genes, *CDKN2C*, *RBI1*, and *TP53* (**Fig. 4**). For *CDKN2C*, the panel detected homozygous deletions in seven of 233 samples which ranged in size from 21.9 to 235.4 kb and

Table 1. Detection rates of CNAs by targeted panel compared with WGS.

Gene	Sensitivity (95% CI)	Specificity (95% CI)	PPV (95% CI)	NPV (95% CI)	Accuracy (95% CI)
<i>CDKN2C</i>	100% (71.51–100)	100% (96.45–100)	100% (N/A)	100% (N/A)	100% (96.79–100)
<i>CKS1B</i>	97.87% (88.71–99.95)	98.55% (92.19–99.96)	97.87% (86.97–99.69)	98.55% (90.72–99.79)	98.28% (93.91–99.79)
<i>RB1</i>	100% (93.51–100)	100% (93.84–100)	100% (N/A)	100% (N/A)	100% (96.79–100)
<i>TP53</i>	100% (83.89–100)	98.91% (94.09–99.97)	95.45% (74.94–99.33)	100% (N/A)	99.12% (95.17–99.98)
All regions	99.25% (95.91–99.98)	99.38% (97.77–99.92)	98.52% (94.35–99.62)	99.69% (97.84–99.96)	99.34% (98.09–99.86)

affected both coding exons of the gene. Of these seven samples, four also had WGS and the homozygous deletions were detected only in one of four.

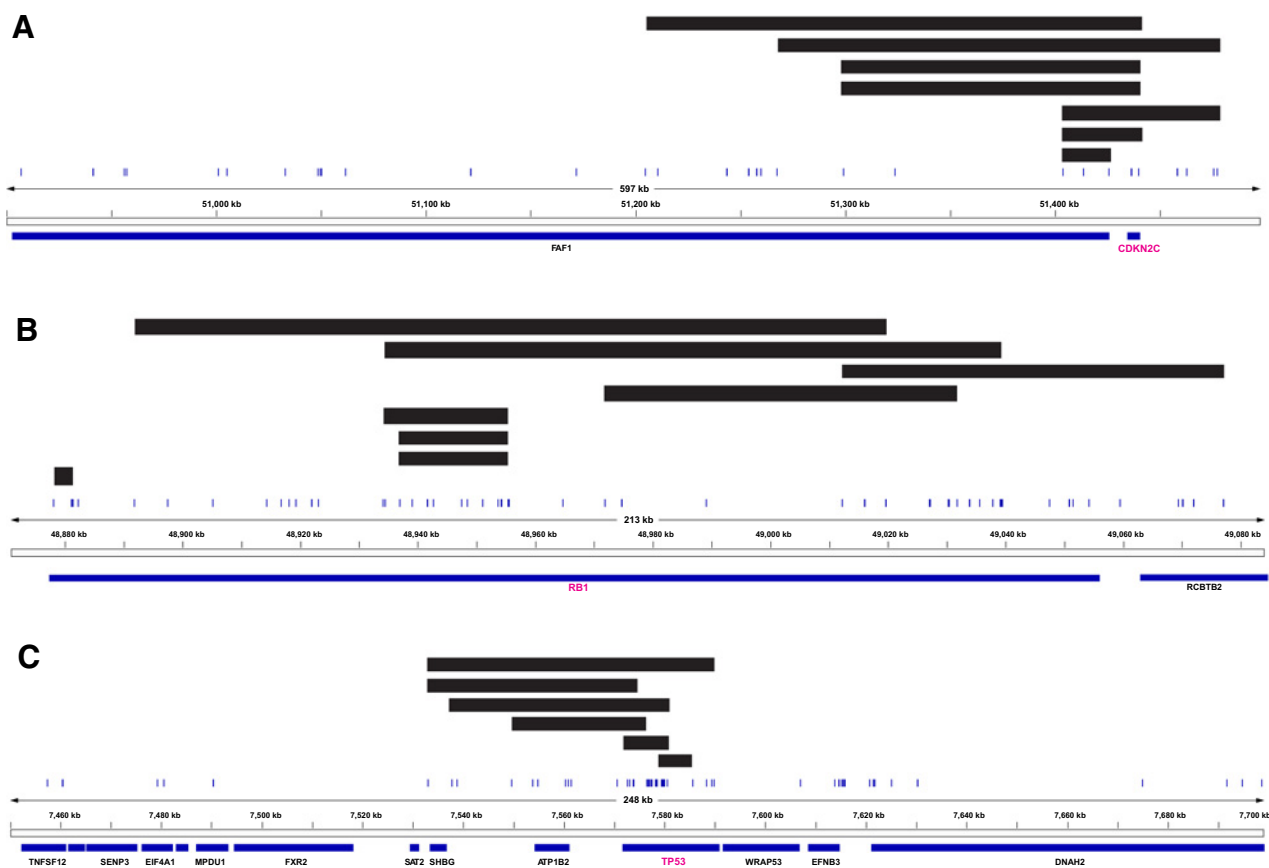
For *RB1*, homozygous deletions were detected in eight of 233 samples and ranged in size from 3.5 to 105.3 kb. WGS was available for four of eight, and a homozygous deletion was detected in one sample. The remaining three samples, where WGS did not detect the deletion, were from the same patient and the deletion was 18.6 kb. None of the homozygous deletions spanned the entire gene with most deleting several exons within the gene. As such, these deletions would be unlikely to be detected by FISH.

For *TP53*, six samples with a homozygous deletion were identified. Of these homozygous deletions, none covered the entire gene. The homozygous deletions ranged in size from 6.1 to 56.8 kb. Three of the

six samples also had WGS, of which only one detected the homozygous deletion. The deletions that were not detected by WGS were 6.1, 8.1, and 27.6 kb in size. Given the small nature of all six homozygous deletions, they are unlikely to be detectable by FISH.

Translocation breakpoint detection and validation

In the 233 patient samples, canonical Ig translocations were detected in 47% of samples, encompassing t(4;14), t(6;14), t(11;14), t(14;16), and t(14;20) in 13%, 4%, 25%, 3%, and 2%, respectively. This is consistent with the expected frequencies of these translocations, with some enrichment of t(4;14) and t(11;14) due to sample selection bias. The distribution of the translocation breakpoints at the IgH locus is shown in Fig. 5 and it aligns with previously published data (38).

**Figure 4.**

Detection of homozygous deletions in the key tumor suppressor genes *CDKN2C* (A), *RB1* (B), or *TP53* (C) loci. Samples with homozygous deletions plotted at the *CDKN2C* (A), *RB1* (B), or *TP53* (C) loci. Black bars indicate homozygous deletion events in samples. Gene/exon locations are shown below each plot and vertical lines indicate capture regions on the panel.

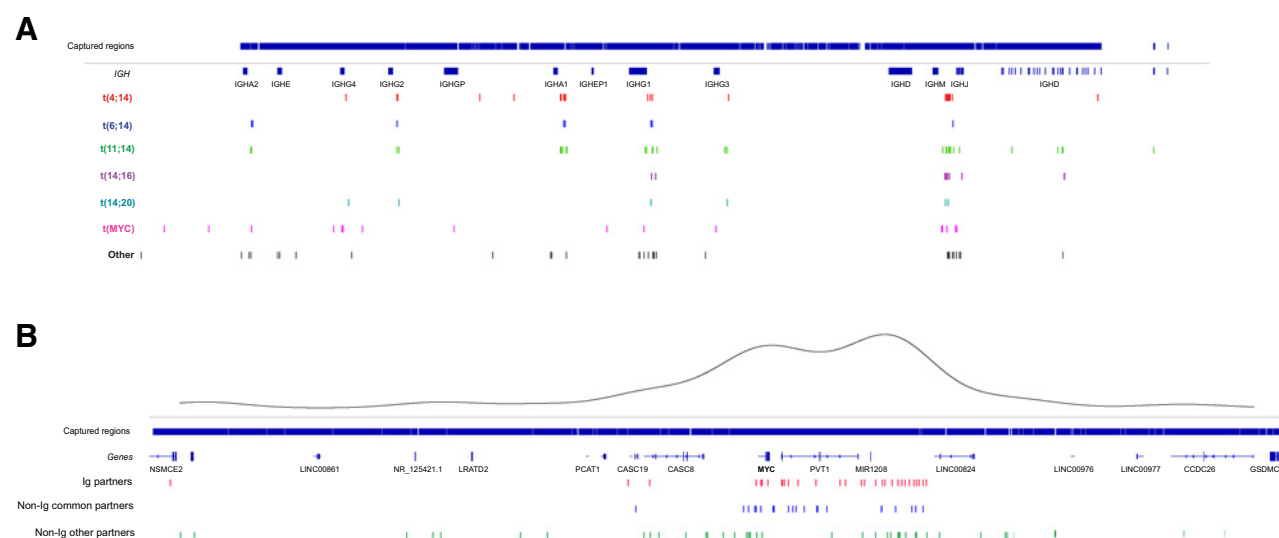


Figure 5.

Translocation breakpoints. **A**, *IGH@* locus breakpoints broken down by partner chromosome. *V* regions not shown for clarity. Captured regions extend to each *V* region. **B**, *MYC* region breakpoints broken down by Ig, non-Ig common (*FOXO3*, *TXNDC5*, *FAM46C*), and other partners. A kernel density plot shows the two main translocation hotspots centromeric of *MYC* and telomeric of *PVT1*.

One hundred and sixteen samples had WGS data available to validate the capture panel results and to ensure that no translocations were missed. There was complete agreement between targeted panel and WGS calls for the canonical translocations: t(4;14) ($n = 19$), t(6;14) ($n = 2$), t(11;14) ($n = 46$), t(14;16) ($n = 3$), t(14;20) ($n = 1$), and no translocation detected ($n = 45$). As the results were completely consistent between the platforms, the sensitivity, specificity, PPV, NPV, and accuracy were all 100% (Table 2).

In addition, clinical FISH data were available for 92 samples. A total of 85 samples gave concordant results between technologies with translocations detected in 56 samples and not observed in 29 samples (Supplementary Table S11). FISH did not detect four translocations that were detected by targeted sequencing and WGS [one t(4;14), one t(14;20), and two t(11;14)], and in three additional samples a rearrangement at the IgH locus was detected by FISH but the partner chromosome was not identified [t(8;14), t(6;14), and t(11;14) detected by targeted panel and WGS]. In one sample a variant t(4;14) was detected by FISH but not by targeted sequencing or WGS. Therefore,

targeted sequencing only failed to detect one variant translocation that was detected by FISH but gave more information on six samples than was given by FISH highlighting the superiority of sequencing approach over FISH methods. The statistical comparisons between the targeted sequencing panel (and also WGS as they were identical) and FISH are shown in Table 2 and Supplementary Table S11.

In addition, since immunoglobulin lambda chain (IgL) rearrangements have been shown to be prognostic in multiple myeloma (43), we examined the detection of these between panel and WGS data. The panel detected IgL translocations in 10 samples, including the most common rearrangement *IgL:MYC* in eight of the samples. Of these 10 samples, seven also had WGS data and were confirmed by that method. WGS sequencing identified nine samples with translocations involving the IgL locus, of which seven were detected by the panel. Of the two discordant samples, one was a t(8;22) and was resolved with realignment to hg38. The other discordant sample had a complex event involving five chromosomes (chr 5, 7, 14, 19, and 22) by WGS, of which three of the breakpoints (chr 7, 14, and 19) were detected by the panel.

Table 2. Detection rates of *IGH* translocations by targeted panel compared with WGS and FISH.

		Sensitivity (95% CI)	Specificity (95% CI)	PPV (95% CI)	NPV (95% CI)	Accuracy (95% CI)
t(11;14)	WGS	100% (92.13–100)	100% (94.72–100)	100% (N/A)	100% (N/A)	100% (96.79–100)
	FISH	100% (90–100)	94.57% (85.38–98.9)	92.11% (79.5–97.23)	100% (N/A)	96.74% (90.77–99.32)
t(4;14)	WGS	100% (81.47–100)	100% (96.19–100)	100% (N/A)	100% (N/A)	100% (96.79–100)
	FISH	94.12% (71.31–99.85)	98.67% (92.79–99.97)	94.12% (69.47–99.12)	98.67% (91.7–99.80)	97.83% (92.37–99.74)
t(6;14)	WGS	100% (15.81–100)	100% (96.73–100)	100% (N/A)	100% (N/A)	100% (96.79–100)
	FISH	N/A	98.91% (94.09–99.97)	N/A	100% (N/A)	N/A
t(14;16)	WGS	100% (29.24–100)	100% (96.7–100)	100% (N/A)	100% (N/A)	100% (96.79–100)
	FISH	100% (29.24–100)	100% (95.94–100%)	100% (N/A)	100% (N/A)	100% (96.07–100)
t(14;20)	WGS	100% (2.5–100)	100% (96.76–100)	100% (N/A)	100% (N/A)	100% (96.79–100)
	FISH	N/A	98.91% (94.09–99.97)	N/A	100% (N/A)	N/A
ALL regions	WGS	100% (94.79–100)	100% (91.96–100)	100% (N/A)	100% (N/A)	100% (96.79–100)
	FISH	94.92% (85.85–98.94)	87.88% (71.8–96.6)	93.33% (84.79–97.23)	90.63% (76.11–96.7)	92.39% (84.95–96.89)

Novel translocation partners detected by targeted sequencing

An advantage of capture panels is that novel events can also be detected. We have previously identified novel translocations to the Ig loci affecting partner proto-oncogenes (39, 44). In this study from 185 samples, we identified novel Ig translocations in 20 samples (10.8%). The partner loci included some known oncogenes such as *CCND2*, *KMT2B*, *PAX5*, *MYCN*, *MAP3K14*, *BCL2*, and *TNFAIP8*, but also identified some potentially novel oncogenes such as *UST*, *TNFSF12*, *DEFB1*, and *LRRK2*. *KMT2B* is also frequently mutated indicating multiple mechanisms of disrupting the gene in oncogenesis. The prognostic significance of these infrequent translocation partners is difficult to ascertain, but they may lead to better understanding of disease biology through identification of new driver genes.

MYC rearrangements and CNAs

We previously performed a comprehensive analysis of *MYC* translocations and CNAs in multiple myeloma using an identical panel design (27). The location of *MYC* translocation breakpoints in this dataset are shown in Fig. 5. The frequency of *MYC* translocations was 24.0% with 49.4% of samples having a CNA within 2 Mb of *MYC*, which we have shown can affect expression of *MYC* (27). Many samples with a translocation also had CNAs and so the total frequency of samples with *MYC* abnormalities was 66.9.1% (156/233; Supplementary Fig. S5).

Validation of *MYC* translocations detected by the panel against WGS data ($n = 116$) showed agreement in 91.4% of samples (106/116). Of the discordant samples ($n = 10/116$), *MYC* translocations were detected by the panel and not by WGS in four samples and were judged to be subclonal translocations with insufficient depth of coverage in the WGS. The remaining six translocations that were only detected by WGS had been filtered out due to mapping quality issues with hg19 alignments and were resolved with realignment to hg38.

Comparison of multiple myeloma targeted sequencing panels

Several other multiple myeloma targeted sequencing panels have been described and are summarized in Table 3 (13, 14, 45–47). Most of those panels could detect mutations, CNAs, and IgH locus rearrangements, however, they were not universally validated using orthogonal technologies. Of these, the Yellapantula and colleagues (47) panel is the most characterized with validation by FISH for translocations and SNP array for CNAs. One key aspect missing from the Yellapantula and colleagues panel is that it only detects *MYC* abnormalities partnered with the *IGH* locus. The MGP panel also has the region surrounding *MYC* on 8q24 assayed, allowing for the detection of non-Ig partners which are more frequent than Ig partners. *MYC* rearrangements have been shown to be prognostic and associated with a shorter time to progression from SMM to symptomatic multiple myeloma (33, 35, 48). MGP is the only panel to be validated against WGS and show comparable identification of mutations, CNAs, and translocations between the methodologies. This comparison indicates that for those laboratories which cannot yet perform WGS on all multiple myeloma samples diagnostically, the MGP panel is a viable, cost-effective, and accurate alternative to generate prognostically meaningful data.

Discussion

WGS of patient samples is increasingly popular in research laboratories and can also be utilized for clinical diagnostics (18). However, the cost, processing time, and high throughput computational expertise required to analyze data can be prohibitive for smaller nonacademic centers. We have developed and validated a sequencing panel that is relevant to prognosis, risk stratification, and treatment of patients with multiple myeloma and have described an end-to-end protocol for laboratory and bioinformatic processing of samples and data visualization. This panel has been utilized, in different forms, for the analysis of SMM, NDMM,

Table 3. Targeted NGS-based assays in multiple myeloma.

Reference	Summary of panel design	MM pts/cell lines (N)	Detection of:				Cross-validation of:		
			SNVs	CNAs	Ig SVs	Non-Ig MYC SVs	SNVs	CNAs	SVs
Kortum and colleagues (46)	Targeted sequencing-semiconductor technology, 47 genes	72 del17p patients	✓	—	—	—	—	—	—
Bolli and colleagues (14)	Capture-based NGS, 246 genes	5 patients/14 cell lines	✓	✓	✓	—	—	—	—
Corre and colleagues (45)	Same as Bolli and colleagues	43 patients	✓	✓	✓	—	—	—	— ^a
White and colleagues (13)	Capture-based NGS, 465 genes	95 patients	✓	✓	✓	✓ ^b	—	—	—
Yellapantula and colleagues (47)	Capture-based NGS, 120 genes	154 patients	✓	✓	✓	—	—	✓	✓
He and colleagues (56)	Foundation Medicine Heme DNA/RNA hybrid capture	1,338 patients	✓	✓	✓	—	✓	✓	✓
Sudha and colleagues (current study)	Capture-based NGS, 228 genes	233 patients/13 cell lines	✓	✓	✓	✓	✓	✓	✓
							Sequenom ddPCR, WGS	NGS MLPA, FISH, WGS	FISH, WGS

Abbreviations: MM, multiple myeloma; pts, patients; SV, structural variant.

^aFISH available for t(4;14) and del(17p), but not directly compared.

^b*MYC* capture region limited to 160 kb.

previously treated multiple myeloma, and PCL patient samples (1, 25, 27, 29, 30, 33, 36, 49). Although not yet extensively used in relapsed refractory multiple myeloma (RRMM), the assay contains regions of interest for this setting, including the p53 pathway (*TP53*, *ATM*, *ATR*, *PRDM1*, and *CRBN* (41, 50). Other common abnormalities can also be detected including exonic deletions of *KDM6A*, deletion of *FGFR3* in t(4;14) samples, and deletions of negative regulators of the NF- κ B pathway, *BIRC2/3*, *TRAF2/3*, and *CYLD*, as well as *NIK* (*MAP3K14*) rearrangements (Supplementary Figs. S6–S9; refs. 51–53). We have formally validated the data generated here against WGS, MLPA, clinical FISH, and mutation standards for translocations, copy number, and mutation identification. In addition, the low input amount of genomic DNA (100 ng) used here allows for the profiling of samples with low disease burden where there are few cells to analyze. We have also successfully performed the assay with only 50 ng of DNA without loss of performance.

For translocation detection we report 100% concordance with WGS data, confirming that WGS is not required for accurate detection of these structural events in multiple myeloma. Furthermore, this assay can be utilized for the detection of translocations in other B-cell malignancies. In addition, we show that *MYC* structural alterations (interchromosomal translocations, CNAs) can be detected with this assay. The breadth and complexity of *MYC* abnormalities have resulted in the underestimation of this locus by FISH, where only 10% to 15% of NDMM samples have the abnormality, whereas targeted sequencing and WGS identifies up to 50% of patients with an abnormality (27, 54).

CNAs were validated against WGS and MLPA, which has been used in clinical trials (21). Compared with MLPA, the panel showed a correlation of $R^2 = 0.987$ and compared with WGS the sensitivity and specificity, were 94.89% and 99.68%, respectively. The main advantage for the panel against WGS was in the detection of small homozygous deletions, where multiple algorithms were required to detect all homozygous deletions in the WGS data. The number of individually analyzed probes in exons and surrounding SNPs in the panel gave more confidence in detecting these small events.

Other targeted panels have been described for the examination of multiple myeloma patient samples (14, 47, 55), but none has been used as extensively or is as exhaustive as the MGP Panel encompassing the three main drivers of multiple myeloma: mutations, CNAs, and translocations (Table 3). We have used the translocation part of the panel as a bolt-on for exome studies (37), before incorporating it into a targeted design, which has now been used in over 550 tumor samples. Previously described targeted panels were not robustly tested nor cross-validated across platforms and laboratories. We have demonstrated the performance of our targeted panel against multiple well-established methods including ddPCR, MLPA, FISH, and WGS. We also provide a complete workflow including a graphical user interface (42) that can be adopted in any laboratory and modified to suit their needs.

The MGP Panel has been adopted for retrospective analysis of clinical trial samples (K.L. Yong; personal communication) and for use in clinical care. Our goal is to broadly share this panel with the multiple myeloma community to improve opportunities and parity across academic and community centers to quickly and easily identify patients with high-risk disease or targetable genetic mutations. Despite several efforts to construct a genomics-based molecular profiling platform in multiple myeloma, this approach has not been broadly

adopted in clinical care nor for improved risk stratification of patients. We encourage the multiple myeloma community (guided by organizations such as IMWG and International Myeloma Society) to seriously consider a thorough examination of the different methods and potentially build consensus around adoption of a molecular-profiling strategy.

Authors' Disclosures

M. Czader reports grants and personal fees from Beckman Coulter outside the submitted work. N. Ansari-Pour reports other support from BMS during the conduct of the study. K.L. Yong reports grants from Amgen during the conduct of the study. W.E. Pierceall reports other support from Bristol Myers Squibb during the conduct of the study. E. Flynt reports other support from Bristol Myers Squibb outside the submitted work. S. Gooding reports grants from Bristol Myers Squibb during the conduct of the study. K. Ramasamy reports grants from Bristol Myers Squibb outside the submitted work. B.A. Walker reports grants from Bristol Myers Squibb and Leukemia and Lymphoma Society during the conduct of the study. No disclosures were reported by the other authors.

Authors' Contributions

P. Sudha: Data curation, formal analysis, validation, investigation, methodology, writing–review and editing. **A. Ahsan:** Data curation, formal analysis, supervision, validation, investigation, methodology, writing–original draft. **C. Ashby:** Data curation, formal analysis, investigation, methodology, writing–review and editing. **T. Kausar:** Data curation, investigation, methodology, writing–review and editing. **A. Khara:** Data curation, formal analysis, writing–review and editing. **M.H. Kazeroun:** Data curation, formal analysis, methodology, writing–review and editing. **C.-C. Hsu:** Investigation, methodology, writing–review and editing. **L. Wang:** Investigation, methodology, writing–review and editing. **E. Fitzsimons:** Data curation, investigation, methodology, writing–review and editing. **O. Salminen:** Data curation, investigation, methodology, writing–review and editing. **M. Czader:** Data curation, investigation, methodology, writing–review and editing. **J. Williams:** Supervision, methodology, writing–review and editing. **M.I. Abu Zaid:** Resources, investigation, methodology, writing–review and editing. **N. Ansari-Pour:** Formal analysis, supervision, methodology, writing–review and editing. **K.L. Yong:** Resources, supervision, writing–review and editing. **F. van Rhee:** Resources, writing–review and editing. **W.E. Pierceall:** Resources, writing–original draft, project administration. **G.J. Morgan:** Resources, supervision, writing–review and editing. **E. Flynt:** Conceptualization, resources, supervision, funding acquisition, investigation, methodology, writing–original draft. **S. Gooding:** Resources, data curation, supervision, investigation, writing–review and editing. **R. Abonour:** Resources, supervision, writing–review and editing. **K. Ramasamy:** Resources, supervision, writing–review and editing. **A. Thakurta:** Conceptualization, resources, supervision, funding acquisition, investigation, methodology, writing–original draft. **B.A. Walker:** Conceptualization, resources, data curation, formal analysis, supervision, funding acquisition, investigation, methodology, writing–original draft.

Acknowledgments

Research support was received from Bristol Myers Squibb. B.A. Walker was partially supported by a grant from the Leukemia and Lymphoma Society and the Daniel and Lori Efroymsen Chair. The Indiana Myeloma Registry is funded in part by support from the Indiana University Precision Health Initiative, Miles for Myeloma, the Harry and Edith Gladstein Chair, and the Omar Barham Fighting Cancer Fund. Computational infrastructure at Indiana University (Indianapolis, IN) was funded in part by Lilly Endowment Inc. through the Indiana University Pervasive Technology Institute. Authors are grateful to Gail Vance and Mirian Salazar for helpful discussions.

The costs of publication of this article were defrayed in part by the payment of page charges. This article must therefore be hereby marked *advertisement* in accordance with 18 U.S.C. Section 1734 solely to indicate this fact.

Received October 19, 2021; revised January 11, 2022; accepted May 3, 2022; published first May 6, 2022.

References

- Walker BA, Mavrommatis K, Wardell CP, Ashby TC, Bauer M, Davies FE, et al. Identification of novel mutational drivers reveals oncogene dependencies in multiple myeloma. *Blood* 2018;132:587–97.
- Szalat R, Munshi NC. Genomic heterogeneity in multiple myeloma. *Curr Opin Genet Dev* 2015;30:56–65.
- Manier S, Salem KZ, Park J, Landau DA, Getz G, Ghobrial IM. Genomic complexity of multiple myeloma and its clinical implications. *Nat Rev Clin Oncol* 2017;14:100–13.
- Manier S, Salem K, Glavey SV, Roccaro AM, Ghobrial IM. Genomic aberrations in multiple myeloma. *Cancer Treat Res* 2016;169:23–34.
- Morgan GJ, Walker BA, Davies FE. The genetic architecture of multiple myeloma. *Nat Rev Cancer* 2012;12:335–48.
- Bolli N, Avet-Loiseau H, Wedge DC, Van Loo P, Alexandrov LB, Martincorena I, et al. Heterogeneity of genomic evolution and mutational profiles in multiple myeloma. *Nat Commun* 2014;5:2997.
- Lohr JG, Stojanov P, Carter SL, Cruz-Gordillo P, Lawrence MS, Auclair D, et al. Widespread genetic heterogeneity in multiple myeloma: implications for targeted therapy. *Cancer Cell* 2014;25:91–101.
- Chapman MA, Lawrence MS, Keats JJ, Cibulskis K, Sougnez C, Schinzel AC, et al. Initial genome sequencing and analysis of multiple myeloma. *Nature* 2011;471:467–72.
- Harding T, Baughn L, Kumar S, Van Ness B. The future of myeloma precision medicine: integrating the compendium of known drug resistance mechanisms with emerging tumor profiling technologies. *Leukemia* 2019;33:863–83.
- Gonzalez-Calle V, Fonseca R. [Towards precision medicine in myeloma: new evidence and challenges]. *Medicina (B Aires)* 2017;77:222–6.
- Erin Flynt AT. Shadow of the Future: Precision medicine in multiple myeloma. *J Precis Med* 2019;5.
- Lagana A, Beno I, Melnekoff D, Leshchenko V, Madduri D, Ramdas D, et al. Precision medicine for relapsed multiple myeloma on the basis of an integrative multiomics approach. *JCO Precis Oncol* 2018;2:PO.18.00019.
- White BS, Lanc I, O'Neal J, Gupta H, Fulton RS, Schmidt H, et al. A multiple myeloma-specific capture sequencing platform discovers novel translocations and frequent, risk-associated point mutations in IGLL5. *Blood Cancer J* 2018;8:35.
- Bolli N, Li Y, Sathiaselan V, Raine K, Jones D, Ganly P, et al. A DNA target-enrichment approach to detect mutations, copy number changes and immunoglobulin translocations in multiple myeloma. *Blood Cancer J* 2016;6:e467.
- Bolli N, Biancon G, Moarii M, Gimondi S, Li Y, de Philippis C, et al. Analysis of the genomic landscape of multiple myeloma highlights novel prognostic markers and disease subgroups. *Leukemia* 2018;32:2604–16.
- Kortum KM, Mai EK, Hanafiah NH, Shi CX, Zhu YX, Bruins L, et al. Targeted sequencing of refractory myeloma reveals a high incidence of mutations in CRBN and Ras pathway genes. *Blood* 2016;128:1226–33.
- Walker BA. Whole exome sequencing in multiple myeloma to identify somatic single nucleotide variants and key translocations involving immunoglobulin Loci and MYC. *Methods Mol Biol* 2018;1792:71–95.
- Hollein A, Twardziok SO, Walter W, Hutter S, Baer C, Hernandez-Sanchez JM, et al. The combination of WGS and RNA-Seq is superior to conventional diagnostic tests in multiple myeloma: Ready for prime time? *Cancer Genet* 2020;242:15–24.
- Yu Y, Brown Wade N, Hwang AE, Nooka AK, Fiala MA, Mohrbacher A, et al. Variability in cytogenetic testing for multiple myeloma: A comprehensive analysis from across the United States. *JCO Oncol Pract* 2020;16:e1169–e80.
- Leeksa AC, Baliakas P, Moysiadis T, Puiggros A, Plevova K, Van der Kevie-Kersemaekers AM, et al. Genomic arrays identify high-risk chronic lymphocytic leukemia with genomic complexity: a multi-center study. *Haematologica* 2021;106:87–97.
- Shah V, Johnson DC, Sherborne AL, Ellis S, Aldridge FM, Howard-Reeves J, et al. Subclonal TP53 copy number is associated with prognosis in multiple myeloma. *Blood* 2018;132:2465–9.
- Palumbo A, Avet-Loiseau H, Oliva S, Lokhorst HM, Goldschmidt H, Rosinol L, et al. Revised International Staging System for multiple myeloma: A report from International Myeloma Working Group. *J Clin Oncol* 2015;33:2863–9.
- Abe Y, Ishida T. Immunomodulatory drugs in the treatment of multiple myeloma. *Jpn J Clin Oncol* 2019;49:695–702.
- Rajkumar SV, Kumar S. Multiple myeloma current treatment algorithms. *Blood Cancer J* 2020;10:94.
- Walker BA, Mavrommatis K, Wardell CP, Ashby TC, Bauer M, Davies F, et al. A high-risk, double-hit, group of newly diagnosed myeloma identified by genomic analysis. *Leukemia* 2019;33:159–70.
- Walker BA, Wardell CP, Brioli A, Boyle E, Kaiser MF, Begum DB, et al. Translocations at 8q24 juxtapose MYC with genes that harbor superenhancers resulting in overexpression and poor prognosis in myeloma patients. *Blood Cancer J* 2014;4:e191.
- Mikulasova A, Ashby C, Tytarenko RG, Qu P, Rosenthal A, Dent JA, et al. Microhomology-mediated end joining drives complex rearrangements and over expression of MYC and PVT1 in multiple myeloma. *Haematologica* 2019;105:1055–66.
- Abdallah N, Baughn LB, Rajkumar SV, Kapoor P, Gertz MA, Dispenzieri A, et al. Implications of MYC rearrangements in newly diagnosed multiple myeloma. *Clin Cancer Res* 2020;26:6581–8.
- Boyle EM, Ashby C, Tytarenko RG, Deshpande S, Wang H, Wang Y, et al. BRAF and DIS3 mutations associate with adverse outcome in a long-term follow-up of patients with multiple myeloma. *Clin Cancer Res* 2020;26:2422–32.
- Ashby C, Tytarenko RG, Wang Y, Weinhold N, Johnson SK, Bauer M, et al. Poor overall survival in hyperhaploid multiple myeloma is defined by double-hit bi-allelic inactivation of TP53. *Oncotarget* 2019;10:732–7.
- Weinhold N, Ashby C, Rasche L, Chavan SS, Stein C, Stephens OW, et al. Clonal selection and double-hit events involving tumor suppressor genes underlie relapse in myeloma. *Blood* 2016;128:1735–44.
- Flynt E, Bisht K, Sridharan V, Ortiz M, Towfic F, Thakurta A. Prognosis, biology, and targeting of TP53 dysregulation in multiple myeloma. *Cells* 2020;9:287.
- Boyle EM, Deshpande S, Tytarenko R, Ashby C, Wang Y, Bauer MA, et al. The molecular make up of smoldering myeloma highlights the evolutionary pathways leading to multiple myeloma. *Nat Commun* 2021;12:293.
- Bustoros M, Sklaventis-Pistofidis R, Park J, Redd R, Zhitomirsky B, Dunford AJ, et al. Genomic profiling of smoldering multiple myeloma identifies patients at a high risk of disease progression. *J Clin Oncol* 2020;38:2380–9.
- Misund K, Keane N, Stein CK, Asmann YW, Day G, Welsh S, et al. MYC dysregulation in the progression of multiple myeloma. *Leukemia* 2020;34:322–6.
- Thanendrarajan S, Tian E, Qu P, Mathur P, Schinke C, van Rhee F, et al. The level of deletion 17p and bi-allelic inactivation of TP53 has a significant impact on clinical outcome in multiple myeloma. *Haematologica* 2017;102:e364–e7.
- Walker BA, Boyle EM, Wardell CP, Murison A, Begum DB, Dahir NM, et al. Mutational spectrum, copy number changes, and outcome: Results of a sequencing study of patients with newly diagnosed myeloma. *J Clin Oncol* 2015;33:3911–20.
- Walker BA, Wardell CP, Johnson DC, Kaiser MF, Begum DB, Dahir NB, et al. Characterization of IGH locus breakpoints in multiple myeloma indicates a subset of translocations appear to occur in pregerminal center B cells. *Blood* 2013;121:3413–9.
- Walker BA, Wardell CP, Ross FM, Morgan GJ. Identification of a novel t(7;14) translocation in multiple myeloma resulting in overexpression of EGFR. *Genes Chromosomes Cancer* 2013;52:817–22.
- Walker BA, Morgan GJ. The genomic features associated with high-risk multiple myeloma. *Oncotarget* 2018;9:35478–9.
- Gooding S, Ansari-Pour N, Towfic F, Estevez MO, Chamberlain PP, Tsai KT, et al. Multiple cereblon genetic changes are associated with acquired resistance to lenalidomide or pomalidomide in multiple myeloma. *Blood* 2021;137:232–7.
- Ashby C, Rutherford M, Bauer MA, Peterson EA, Wang Y, Boyle EM, et al. TarPan: an easily adaptable targeted sequencing panel viewer for research and clinical use. *BMC Bioinf* 2020;21:144.
- Barwick BG, Neri P, Bahlis NJ, Nooka AK, Dhodapkar MV, Jaye DL, et al. Multiple myeloma immunoglobulin lambda translocations portend poor prognosis. *Nat Commun* 2019;10:1911.
- Morgan GJ, He J, Tytarenko R, Patel P, Stephens OW, Zhong S, et al. Kinase domain activation through gene rearrangement in multiple myeloma. *Leukemia* 2018;32:2435–44.
- Corre J, Cleynen A, du Pont SR, Buisson L, Bolli N, Attal M, et al. Multiple myeloma clonal evolution in homogeneously treated patients. *Leukemia* 2018;32:2636–47.
- Kortum KM, Langer C, Monge J, Bruins L, Zhu YX, Shi CX, et al. Longitudinal analysis of 25 sequential sample-pairs using a custom multiple myeloma mutation sequencing panel (M(3)P). *Ann Hematol* 2015;94:1205–11.
- Yellapantula V, Hultcrantz M, Rustad EH, Wasserman E, Londono D, Cimera R, et al. Comprehensive detection of recurring genomic abnormalities: a targeted sequencing approach for multiple myeloma. *Blood Cancer J* 2019;9:101.

48. Walker BA, Wardell CP, Murison A, Boyle EM, Begum DB, Dahir NM, et al. APOBEC family mutational signatures are associated with poor prognosis translocations in multiple myeloma. *Nat Commun* 2015;6:6997.
49. Schinke C, Boyle EM, Ashby C, Wang Y, Lyzogubov V, Wardell C, et al. Genomic analysis of primary plasma cell leukemia reveals complex structural alterations and high-risk mutational patterns. *Blood Cancer J* 2020;10:70.
50. Ziccheddu B, Biancon G, Bagnoli F, De Philippis C., Maura F, Rustad EH, et al. Integrative analysis of the genomic and transcriptomic landscape of double-refractory multiple myeloma. *Blood Adv* 2020;4:830–44.
51. van Haafden G, Dalglish GL, Davies H, Chen L, Bignell G, Greenman C, et al. Somatic mutations of the histone H3K27 demethylase gene UTX in human cancer. *Nat Genet* 2009;41:521–3.
52. Keats JJ, Maxwell CA, Taylor BJ, Hendzel MJ, Chesi M, Bergsagel PL, et al. Overexpression of transcripts originating from the MMSET locus characterizes all t(4;14)(p16;q32)-positive multiple myeloma patients. *Blood* 2005;105:4060–9.
53. Demchenko YN, Glebov OK, Zingone A, Keats JJ, Bergsagel PL, Kuehl WM. Classical and/or alternative NF-kappaB pathway activation in multiple myeloma. *Blood* 2010;115:3541–52.
54. Sharma N, Smadbeck JB, Abdallah N, Zepeda-Mendoza C, Binder M, Pearce KE, et al. The prognostic role of MYC structural variants identified by NGS and FISH in multiple myeloma. *Clin Cancer Res* 2021;27:5430–9.
55. Kortum KM, Langer C, Monge J, Bruins L, Egan JB, Zhu YX, et al. Targeted sequencing using a 47 gene multiple myeloma mutation panel (M (3) P) in -17p high risk disease. *Br J Haematol* 2015;168:507–10.
56. He J, Abdel-Wahab O, Nahas MK, Wang K, Rampal RK, Intlekofer AM, et al. Integrated genomic DNA/RNA profiling of hematologic malignancies in the clinical setting. *Blood* 2016;127:3004–14.